Title
The Remarkably Featureless High-Resolution X-Ray Spectrum of Markarian 478

Journal
The Astronomical Journal, 125(2)

ISSN
0004-6256

Authors
Marshall, Herman L
Edelson, Rick A
Vaughan, Simon
et al.

Publication Date
2003-02-01

DOI
10.1086/345820

Peer reviewed

The Remarkably Featureless High Resolution X-ray Spectrum of Mrk 478

Herman L. Marshall[1], Rick A. Edelson[2,3], Simon Vaughan[3,4], Mathew Malkan[2], Paul O'Brien[3], Robert Warwick[3]

hermanm@space.mit.edu, rae@astro.ucla.edu, sav@ast.cam.ac.uk, malkan@astro.ucla.edu, pto@star.le.ac.uk, rsw@star.le.ac.uk

Received _____; accepted _____

To appear in the Astronomical Journal

[1]Center for Space Research, Massachusetts Institute of Technology, 77 Massachusetts Ave., Cambridge, MA 02139

[2]UCLA Astronomy Department, Los Angeles, CA 90095-1562

[3]X-Ray Astronomy Group, University of Leicester, Leicester LE1 7RH, U. K.

[4]Institute of Astronomy, Madingly Road, Cambridge CB3 0HA, U. K.

ABSTRACT

An observation of Mrk 478 using the *Chandra* Low Energy Transmission Grating Spectrometer is presented. The source exhibited 30-40% flux variations on timescales of $\sim 10^4$ s together with a slow decline in the spectral softness over the full 80 ks observation. The 0.15–3.0 keV spectrum is well fitted by a single power law with photon index $\Gamma = 2.91 \pm 0.03$. Combined with high energy data from *BeppoSAX*, the spectrum from 0.15 to 10 keV is well fit as the sum of two power laws with $\Gamma = 3.03 \pm 0.04$, which dominates below 2 keV and 1.4 ± 0.2, which dominates above 2 keV (quoting 90% confidence uncertainties). No significant emission or absorption features are detected in the high resolution spectrum, supporting our previous findings using the Extreme Ultraviolet Explorer but contradicting the claims of emission lines by Hwang & Bowyer (1997). There is no evidence of a warm absorber, as found in the high resolution spectra of many Sy 1 galaxies including others classified as narrow line Sy 1 galaxies such as Mrk 478. We suggest that the X-ray continuum may result from Comptonization of disk thermal emission in a hot corona through a range of optical depths.

Subject headings: galaxies:active — galaxies: individual (Mrk 478)

1. Introduction

High resolution spectra of active galaxies have proven to be a valuable probe of the physical processes governing the gas near their nuclei. The *Chandra* spectra of NGC 4151 (Ogle et al. 2000) and Mrk 3 (Sako et al. 2000), sources in which our direct line of sight to the nucleus is subject to heavy absorption, are characterized by strong emission lines from hot photoionized plasmas located in the extended narrow-line regions of these galaxies.

For an overview of the *Chandra* X-ray Observatory and its complement of instruments, see (Weisskopf et al. 2002). In the spectra of the broad line Sy 1 galaxies (BLS1s) NGC 5548 Kaastra et al. (2000), MCG-6-30-15 (Lee et al. 2001), and NGC 3783 (Kaspi et al. 2000), the more directly observed power law continuum may be absorbed by highly ionized gas that is probably associated with the broad line region.

Narrow line Seyfert 1 galaxies (NLS1s) differ from these BLS1s in that they have narrower optical emission lines and steeper soft X-ray continua, which are usually highly variable. See Osterbrock & Pogge (1985) for observational criteria that define NLS1s. Pounds, Done, and Osborne (1995) and others have suggested that the the accretion rates in NLS1s are closer to the Eddington limit than in BLS1s of the same luminosities. The high resolution *Chandra* grating spectra of the NLS1 galaxies, Ton S 180 (Turner et al. 2001) and NGC 4051 (Collinge et al. 2001), do not yet provide a consistent picture of NLS1s. NGC 4051 has a few emission and absorption lines on a complex continuum, while the X-ray spectrum of Ton S 180 is relatively featureless. *XMM-Newton* Reflection Grating Spectrometer (den Herder et al. 2001, RGS) observations of NLS1s have shown broad absorption troughs attributed to L shell transitions of weakly ionized Fe in two cases: IRAS 13349+2438 (Sako et al. 2001) and Mrk 359 (O'Brien et al. 2001). Further high resolution spectra of NLS1s are needed to clarify the relation between this class of source and their broad-line counterparts.

Mrk 478 is a classic example of the NLS1 class with a strong steep X-ray spectrum (Gondhalekar et al. 1994) and low interstellar column density (N_H). These attributes combine to make it one of the brightest NLS1s in the extreme ultraviolet (EUV, $E \sim 0.1$ keV) (Marshall et al. 1995). The spectrum measured by *EUVE* remains somewhat controversial: Marshall et al. (1996) modelled it with a steep power law spectrum with $N_H \sim 10^{20}$ cm^{-2} but Hwang and Bowyer (1997) later claimed that it showed strong

emission lines at 79 and 83Å in the rest frame. These differences may have resulted from the poor statistical significance of the spectral data. Marshall et al. (1996) argued that the rapid, high amplitude EUV variability of Mrk 478, coupled with weak UV variability indicated that the EUV to soft X-ray portion of the spectrum was the result of Comptonized thermal emission near the inner edge of an accretion disk. The *EUVE* data, however, were insufficient to test for spectral variability or to search for features in the variability spectrum on time scales of less than a few hours.

2. Observations and Data Reduction

Mrk 478 was observed with the Chandra Low Energy Grating Spectrometer (LETGS) using the High Resolution Camera on 8-9 August 2000 (TJD = JD - 2451000. = 765.31-766.27). The exposure time was 80857 s. Nearly simultaneous observations were obtained with BeppoSAX Medium Energy Concentrator Spectrometer (MECS) (Boella et al. 1997) from TJD 766.07 through 767.59.

2.1. LETGS Spectral and Broad-band Variability

The average, background-subtracted count rate in zeroth order was 0.409 ± 0.002 count s^{-1} in a 11″ radius aperture which contains > 99% of the power. Background was determined from a similarly sized region 26″ away from zeroth order in a direction avoiding the dispersed spectra and the diffraction spikes caused by the LETG coarse and fine support structure. The count rate in 300 s bins varied by 30-40% over the observation (see Fig. 1). The dispersed events were binned in 4000 s intervals in order to determine a softness ratio, $R \equiv (S-H)/(S+H)$, where H and S are the counts in hard (5-25 Å, or about 0.5-2.5 keV) and soft (25-60 Å, 0.2-0.5 keV) bands. The uncertainties were determined from counting

statistics only.

The total count rate light curve showed variability on short time scales. Assuming that the variations follow a Gaussian distribution with standard deviation s about the mean count rate R, then the fractional variability amplitude is $F_{var} = s/R = 0.132 \pm 0.008$ after accounting for Poisson fluctuations (Edelson et al. 2002). The strongest event was an increase of almost a factor of 2 in just 20 ksec. The softness ratio also showed a clear trend, decreasing by about 25% throughout the observation. However, this slow trend is not obviously correlated with any of the rapid variations in the total count rate. Fitting spectra to the first and last 10000 s of the observation gives photon indices that changed from 3.02 $\pm$ 0.05 to 2.82 $\pm$ 0.05 over the course of the observation (fixing the column density to the best-fit value).

2.2. LETGS Spectroscopic Data Reduction

The LETGS spectral data were reduced from standard L1 event lists using IDL and custom processing scripts. The procedure is quite similar to standard processing using CIAO and is described in more detail by Marshall et al. (2002). The position of zeroth order was used to locate the standard "bow-tie" extraction region. The effective area (EA) of the LETGS has undergone a few revisions since launch both due to a recalculation of the LETG efficiencies and due to a series of in-flight calibration observations designed to probe the HRC-S quantum efficiency. We adjusted the EA as described in the appendix, which provides a good fit to the spectrum of PKS 2155-304 to a power law model.

Based on a simple model of the spectrum (see the next section), high order fluxes are negligible for $E > 0.15$ keV. In the 0.10-0.15 keV range where high orders are important, the high order spectra are generally smooth so that it is still possible to detect emission or

absorption lines. Based on the analysis in the appendix, the systematic uncertainties in the high order contributions are estimated to be $\sim 10\%$ for $E > 0.13$ keV, where high orders contribute less than half of the observed flux.

2.3. Continuum Fits

The LETGS data were rebinned adaptively to provide a signal/noise ratio of 5 in each bin over the 0.15 to 10.0 keV range (see Fig. 2). Using the adjusted EA model, the spectrum was well fitted by a simple power law with a photon index of 2.91 ± 0.03. Fit parameters are summarized in table 1. The reduced χ^2 was 1.022 for 891 degrees of freedom, which is an acceptable fit even without adding possible systematic errors. The quoted uncertainties are 90% for one interesting parameter; the uncertainties in N_H and Γ were highly correlated so the joint uncertainties are somewhat larger. This model was used as the basis for line searches in the LETGS data.

A single power law model was a bad fit to the LETGS and MECS data jointly. Combining a more coarsely binned LETGS spectrum (to a signal/noise ratio of 20) with the MECS data, the minimum χ^2 was 439 for 152 degrees of freedom for model consisting of a single power law (see table 1). The main deviations are found at high energies as the spectrum flattens in the 2-10 keV band; $\Gamma = 1.98\pm 0.03$ was determined from *ASCA* observations (Reeves & Turner 2000). For the MECS data alone, we obtain $\Gamma = 2.2\pm 0.2$, comparable to the *ASCA* results and significantly flatter than the slope obtained from the LETGS data alone. The X-ray spectrum from 0.15-10.0 keV is best fit by the sum of two power laws with photon indices of 3.03 ± 0.04 and 1.4 ± 0.2 (see Fig. 3). The joint confidence region for the two power law indices is shown in Fig. 4. The steep spectral slope of the soft band is comparable to previous results. Using *EUVE* data in the wavelength range 65-120Å (about 0.1-0.2 keV), Marshall et al. (1996) obtained a slope of 4.2 ± 0.7.

(Gondhalekar et al. 1994) also found a steep photon index ($3.32^{+0.25}_{-0.13}$) using ROSAT PSPC data from the 0.11-1.9 keV band. The Galactic N_H measured by 21 cm absorption (Murphy, Lockman, Laor, & Elvis 1996) is $9.6 \pm 1.0 \times 10^{19}$, which is consistent with the fit results.

2.4. Emission and Absorption Line Searches

The LETGS spectrum was binned at 0.025 Å, which is half of the instrument resolution. No significant features were found that were consistent with the instrument line response. The data were rebinned at 0.125Å to create a count spectrum at slightly coarser resolution (Fig. 5) with sufficient counts per bin to search for narrow spectral features against the continuum model. In order to allow $< 5\%$ chance of a random line detection, features must be more significant than 4.0σ, given that about 790 bins are examined (in the 1-100 Å band shown in Fig. 5. The one bin exceeding this threshold is in the C-K edge where the EA has a systematic error. We conclude that there are no significant, narrow absorption or emission features in the spectrum. At specific wavelengths, we can reduce the significance level threshold because there aren't as many bins tested. We derived 3σ limits to the equivalent widths of unresolved lines (FWHM $\leq$ 0.05 Å): 0.20 Å (800 eV) at Fe-Kα, 0.10 Å for the 4-90 Å range and 0.035 Å in the 6-35 Å range.

Finally, we searched for broader lines, particularly in the EUV region where Hwang and Bowyer (1997) reported 1-2Å wide lines at 79 and 83 Å in the rest frame with fluxes of 4.8 and 2.5 $\times 10^{-4}$ ph cm^{-2} s^{-1}. The line detections were claimed to be significant at the 2.8 and 3.6 σ level, respectively. In order to search for these features in the Chandra spectrum, the putative lines were modeled as Gaussians with $\sigma = 0.5$ Å. Using the best fit power law model and the high order efficiencies, we computed the high order contributions and subtracted them to produce a spectrum representative of first order only. This spectrum was binned to 0.5 Å resolution in order to search for lines that might be ~ 1 Å wide. Fig. 6

shows that any lines with $\lambda > 60$Å must be rather weak. We can place conservative 3σ upper limits to lines 1 Å wide at 1.0×10^{-4} ph cm^{-2} s^{-1} in the 60-100 Å range.

3. Discussion and Summary

The LETGS data can give confidence to an extrapolation from the EUV into the X-ray band, as indicated from simultaneous observations with IUE, EUVE, and ASCA Marshall (2002). It seems rather clear now that the peak of the spectral energy distribution is in the EUV band, as suggested by Marshall et al. (1996). The thermal peak of disk emission is limited to less than 0.1 keV in order that there be no significant spectral curvature in the LETGS spectrum above 0.2 keV. Thus, we may place a limit on the blackbody temperature of $kT \lesssim 0.03$ keV.

The power law shape in the .15-10 keV band can be obtained by Comptonizing the disk thermal emission as suggested by Pounds, Done, and Osborne (1995) in a disk corona. We modelled the disk spectrum as a blackbody at kT_d =20 eV and set the coronal electron temperature to $kT_c \sim 40$ keV. Using the `comptt` model (Titarchuk 1994) in *Xspec*, we estimate that the optical depth can be of ~ 0.5 in order to obtain the rather steep spectral slope below 1 keV. Above 1 keV, the flatter spectrum can be reproduced with the same input spectrum and Comptonizing region but with a somewhat larger optical depth, ~ 5. In reality, there would likely be a wide range of optical depths. The relative strengths of the two components would depend entirely on the relative covering fractions; in this case, the higher optical depth region should be $\sim$1% of the covering fraction in at lower optical depth. Alternatively, Hubeny, et al. (2001) found that self-Comptonized disk atmospheres consisting of H and He can have steep soft spectra for black hole masses $M \sim 10^8$ M$_\odot$. Disk atmospheres with significant metal content would be expected to show absorption edges that are not observed and have somewhat flatter spectra (Ross, Fabian, & Mineshige 1992).

The spectrum of a Comptonized disk should drop exponentially near 1 keV (Hubeny et al.) but this is where a hard power law component begins to dominate, which would result from Comptonization of the disk emission by a very hot corona.

It is interesting that the softness ratios vary on relatively long time scales for both NLS1s and BLS1s. In BLS1s, the spectra tend to soften as they brighten. This has been taken to indicate that a relatively slowly varying soft component, possibly direct emission from an accretion disk, contributes to the soft X-ray spectra of BLS1s. In Mrk 478 and in the NLS1s Akn 564 and Ton S180 (Edelson et al. 2002), however, the total count rate is rapidly variable and appears to be uncorrelated with the softness ratio. The spectral modelling suggests that the entire X-ray spectrum is governed by Compton scattering of thermal emission from the accretion disk. In the covering fraction model, the spectral shapes are dependent primarily on the structure of the corona, which is substantially larger than the hottest regions of the accretion disk, so the spectral shape can vary slowly as the seed photon rate varies. In the disk self-Comptonization model, however, the Comptonizing region is intimately linked to the photon source via the vertical structure of the disk. It would seem unlikely that this vertical structure would vary slowly as the accretion rate through the disk changes rapidly.

We find no narrow emission or absorption features. In particular, we do not detect emission lines at 79 and 83Å that were reported by Hwang and Bowyer (1997) using the same *EUVE* data used by Marshall et al. (1996) to fit a simple continuum model. Similarly, none of the forbidden lines found in the NGC 4051 spectrum are detected in our spectrum; the limit on the Si XIII line at 6.741 Å is consistent with the equivalent width of this line in NGC 4051 but the Ne IX line is at least 50% weaker (with a limit of 0.025 Å) and the O VII 22.102 Å line is $\times 6$ weaker than their counterparts in NGC 4051. Collinge et al. (2001) show that the lines observed in the NGC 4051 X-ray spectrum could result from a

warm absorption system as found in many broad line Sy 1 galaxies (Reynolds 1997). The NLS1 Akn 564 also shows signs of a warm absorber (Matsumoto, Leighly, and Marshall 2001). For Mrk 478, however, we find no evidence of warm absorption that would link this source to other NLS1s, so warm absorption is not a characteristic that can be used to distinguish broad and narrow line Sy 1 galaxies. One NLS1 which has a spectrum similar to that of Mrk 478 is PKS 0558-504. The RGS spectrum O'Brien et al. (2001) shows no significant absorption or emission line features in the 0.3-2 keV band. Instead of fitting the soft spectrum to a power law shape, they used a combination of several blackbody spectra.

Support for this work was provided by the National Aeronautics and Space Administration (NASA) through Chandra Award Number NAG 5-10032 issued by the Chandra X-Ray Center (CXC), which is operated by the Smithsonian Astrophysical Observatory for and on behalf of NASA under contract NAS 8-39073. HLM was supported under NASA contract SAO SV1-61010 for the CXC.

A. Assessing and Adjusting the LETGS Effective Area

We started with the LETGS effective area (EA) that was released by the Chandra X-ray Center on 9 Mar 2000 and updated 31 Oct 2000.[5] The LETG efficiencies were used, along with the transmission models of the UV ion shield, to determine the EAs for orders 2-5.

The EAs were adjusted based on an analysis of the LETGS spectrum of PKS 2155-304, observation ID 331. The spectrum of PKS 2155-304 was well fitted by a power law with a

[5]The effective area is available at `http://cxc.harvard.edu/cal/Links/Letg/User/Hrc_QE/EA/correct_ea/letgs_NOGAP_EA_001031.mod`.

photon index of 2.45 for energies in the 0.5 to 3 keV range, so the model was extrapolated below 0.5 keV to examine the accuracy of calibration near and below the C-K edge. A very good fit with systematic errors of less than 10% could be obtained with slight adjustments to the 1st order EA model; decreasing the optical depth at C-K (0.285 keV) by 0.13 and adding an edge at 75 Å (0.162 keV) with an optical depth of 0.4. The 75 Å edge is an approximate description for an EA adjustment that has now been added to the LETGS EA model but it is not a physical one. This wavelength merely corresponds to a point where the low energy calibration based on HZ 43 was joined to a high energy calibration based on PKS 2155-304 (Pease, et al. 2002).

Higher order efficiencies in 2nd, 3rd, and 4th orders were adjusted by factors of 0.5, 0.8, and 1.8, respectively, in order to match the C-K edge features of 2nd and 3rd orders (at about 87 Å and 130 Å, respectively) and to match the overall count spectrum in the 0.1-0.15 keV band (where these orders dominate). We included 5th order, which was always less than 10% of the observed counts for $E > 0.1$ keV and ignored all higher orders. There were significant residuals in the LETGS spectra of both PKS 2155-304 and Mrk 421 (observation ID 1715) at the C-K edge in first order, however, due to a 0.5 eV error in the energies of the resonance features (resulting from a flight filter wavelength calibration inaccuracy) as described by Pease, et al. (2002).

For an observation of exposure time T, the net count spectrum, C_λ, in a $\delta\lambda$ interval about λ (determined for first order) is given by

$$C_\lambda = T\delta\lambda \sum_{m=0}^{\infty} m N_{\lambda/m} A_m(\lambda/m), \tag{A1}$$

where λ/m is the wavelength in order m that disperses to the same physical location as λ in first order, N_λ is the photon flux at λ, and $A_m(\lambda)$ is the EA in order m at λ. The spectrum shown in Fig. 7 was computed using

$$n_\lambda = \frac{C_\lambda}{TA_\lambda \delta\lambda} \tag{A2}$$

$$= N_\lambda + \sum_{m=2}^{\infty} mN_{\lambda/m} \frac{A_m(\lambda/m)}{A_\lambda} \ , \tag{A3}$$

where $A_\lambda = A_1\lambda$, so n_λ is actually an estimate of N_λ, differing only in the inclusion of higher orders. The contributions to the observed flux densities calculated using eq. A2 due to order m at first order wavelength λ are

$$n_{\lambda,m} = mN_{\lambda/m} \frac{A_m(\lambda/m)}{A_\lambda} \ . \tag{A4}$$

This procedure results in an "unfolded" spectrum in which the computed flux density follows the true flux density closely in the spectral region where first order dominates; i.e., where

$$n_\lambda \gg \sum_{m=2}^{\infty} n_{\lambda,m} \ . \tag{A5}$$

In spectral fitting, eq. A1 is solved iteratively for N_λ or the parameters of a model giving N_λ. We perform all model fits this way and then use eqs. A2 and A4 for visualization purposes.

REFERENCES

Boella, G. et al. 1997, A&AS, 122, 327

Collinge, M. J. et al. 2001, ApJ, 557, 2

den Herder, J. W. et al. 2001, A&A, 365, L7

Edelson, R. E., Turner, T.J., Pounds, K., Vaughan, S., Markowitz, A., Marshall, H.L., Dobbie, P., and Warwick, R., 2002, ApJ, 568, 610

Gondhalekar, P., et al. 1994, MNRAS, 268, 973

Hwang, C.-Y. & Bowyer, S. 1997, ApJ, 475, 552

Hubeny, I., Blaes, O., Krolik, J. H., & Agol, E. 2001, ApJ, 559, 680

Kaastra, J. S., Mewe, R., Liedahl, D. A., Komossa, S., & Brinkman, A. C. 2000, A&A, 354, L83

Kaspi, S., Brandt, W. N., Netzer, H., Sambruna, R., Chartas, G., Garmire, G. P., & Nousek, J. A. 2000, ApJ, 535, L17

Lee, J.C., Ogle, P.M., Canizares, C.R., Marshall, H.L., Schulz, N.S., Morales, R., Fabian, A.C., Iwasawa, K., 2001, ApJ, in press

Marshall, H.L., Fruscione, A., and Carone, T.E., 1995, ApJ, 439, 90

Marshall, H.L., Carone, T.E., Shull, J.M., Malkan, M.A., and Elvis, M. 1996, ApJ, 457, 169

Marshall, H.L. and Schulz, N.S. 2002, ApJ, submitted

Marshall, H.L. 2002, to appear in "Continuing the Challenge of EUV Astronomy: Current Analysis and Prospects for the Future", ASP Conference Series, eds S. Howell, J. Dupuis, D. Golombek, and J. Cullison

Matsumoto, C., Leighly, K. M., and Marshall, H. L. 2001 to appear in *X-ray Emission from Accretion onto Black Holes*, Eds.: T. Yaqoob and J.H. Krolik

Murphy, E. M., Lockman, F. J., Laor, A., & Elvis, M. 1996, ApJS, 105, 369

O'Brien, P. T., Page, K., Reeves, J. N., Pounds, K., Turner, M. J. L., & Puchnarewicz, E. M. 2001, MNRAS, 327, L37

O'Brien, P. T., et al. 2001, A&A, 365, L122

Ogle, P. M., Marshall, H. L., Lee, J. C., and Canizares, C. R. 2000, ApJ, 545, L51

Osterbrock, D. E. & Pogge, R. W. 1985, ApJ, 297, 166

Pease, D., et al. 2002, Proceedings SPIE, in press

Pounds, K., Done, C. & Osborne, J. 1995, MNRAS, 277, L5

Reeves, J. N. & Turner, M. J. L. 2000, MNRAS, 316, 234

Reynolds, C. S. 1997, MNRAS, 286, 513

Ross, R. R., Fabian, A. C., & Mineshige, S. 1992, MNRAS, 258, 189

Sako, M., Kahn, S. M., Paerels, F., & Liedahl, D. A. 2000, ApJ, 543, L115

Sako, M. et al. 2001, A&A, 365, L168

Titarchuk, L. 1994, ApJ, 434, 570

Turner, T. J. et al. 2001, ApJ, 548, L13

Weisskopf, M. C., Brinkman, B., Canizares, C., Garmire, G., Murray, S., & Van Speybroeck, L. P. 2002, PASP, 114, 1

This manuscript was prepared with the AAS LaTeX macros v5.0.

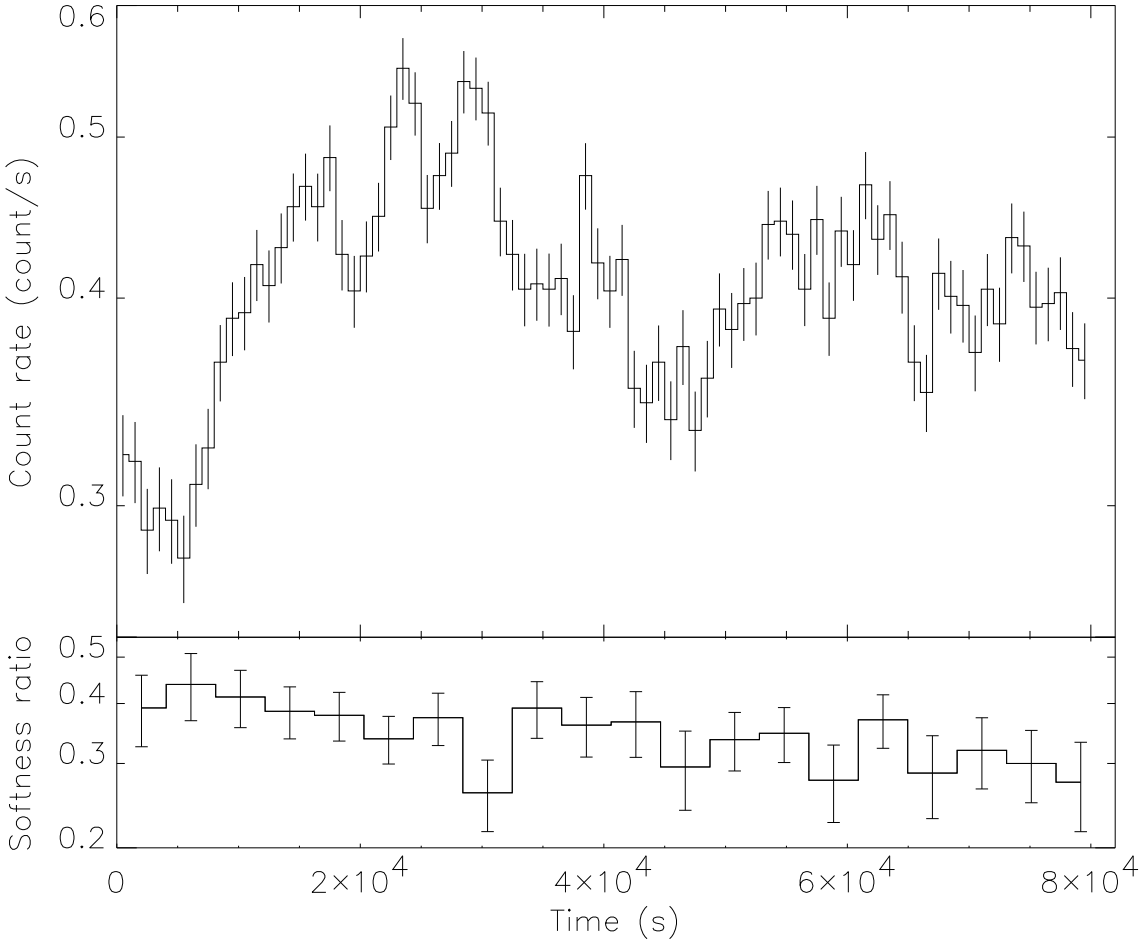

Fig. 1.— *Top:* The light curve of Mrk 478 for the LETGS observation in 300 s intervals derived from the zeroth order data; *bottom:* the softness ratio in 10000 s time intervals using the dispersed events. The effective bandpass of the light curve is 0.2-2.5 keV. The softness ratio is defined as $R = (S - H)/(S + H)$, where H is the count rate in the 5-25 Å (0.5-2.5 keV) band and S is defined as the count rate in the 25-60 Å (0.2-0.5 keV) band. There is a gradual decrease in the softness ratio as the total count rate varies sporadically on a much shorter time scale.

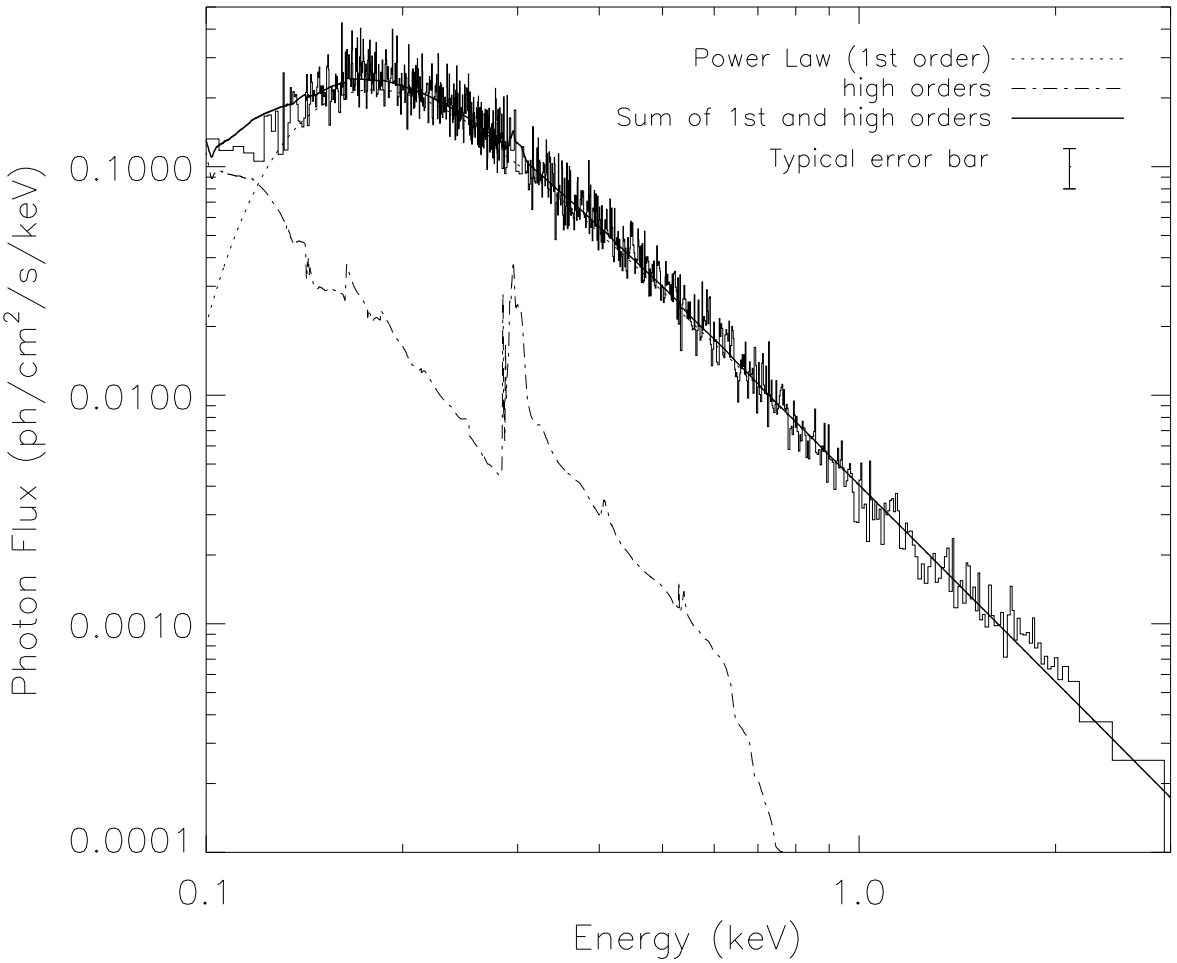

Fig. 2.— The LETGS spectrum of Mrk 478. The bin sizes have been varied to provide a signal/noise ratio of 5 in each bin. *Dotted line:* a power law model of the continuum contribution from first order only, with absorption by cold interstellar material. *Dashed-dotted line:* model of the contribution from orders 2-5, which are negligible for $E > 0.15$ keV. *Solid line:* total of first and high orders, which is an excellent fit to the data.

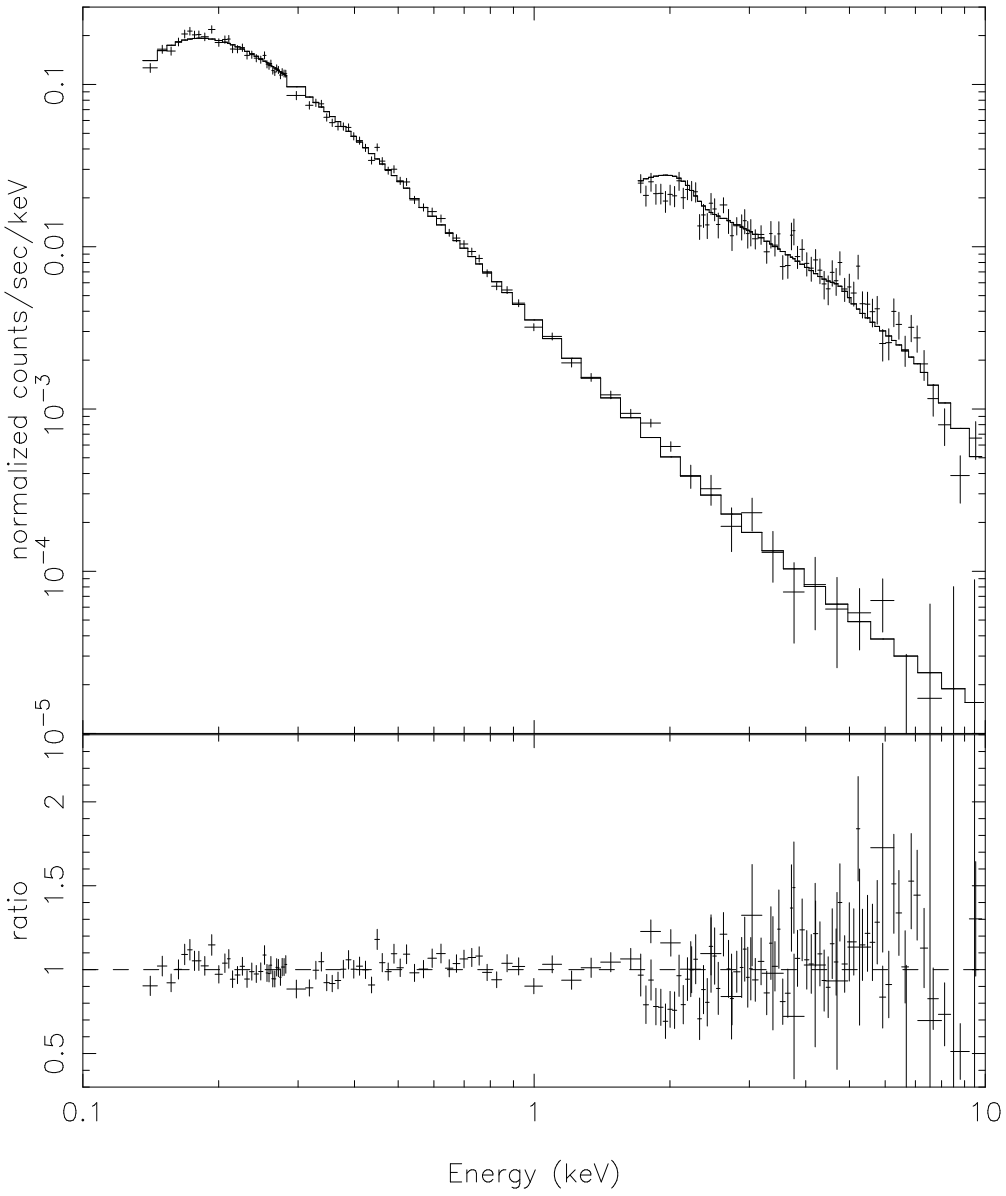

Fig. 3.— The LETGS (left) and MECS (right) spectra of Mrk 478 (*top panel*) and the residuals from the best fit model (*bottom panel*). The LETGS data (spanning 0.15 to 10 keV) were rebinned to provide a signal/noise ratio of 20 in each bin or a maximum binwidth of 5% and were corrected by the estimated contributions of high orders (see Fig. 2). The model consists of the sum of two power laws with absorption by cold interstellar material (see table 1).

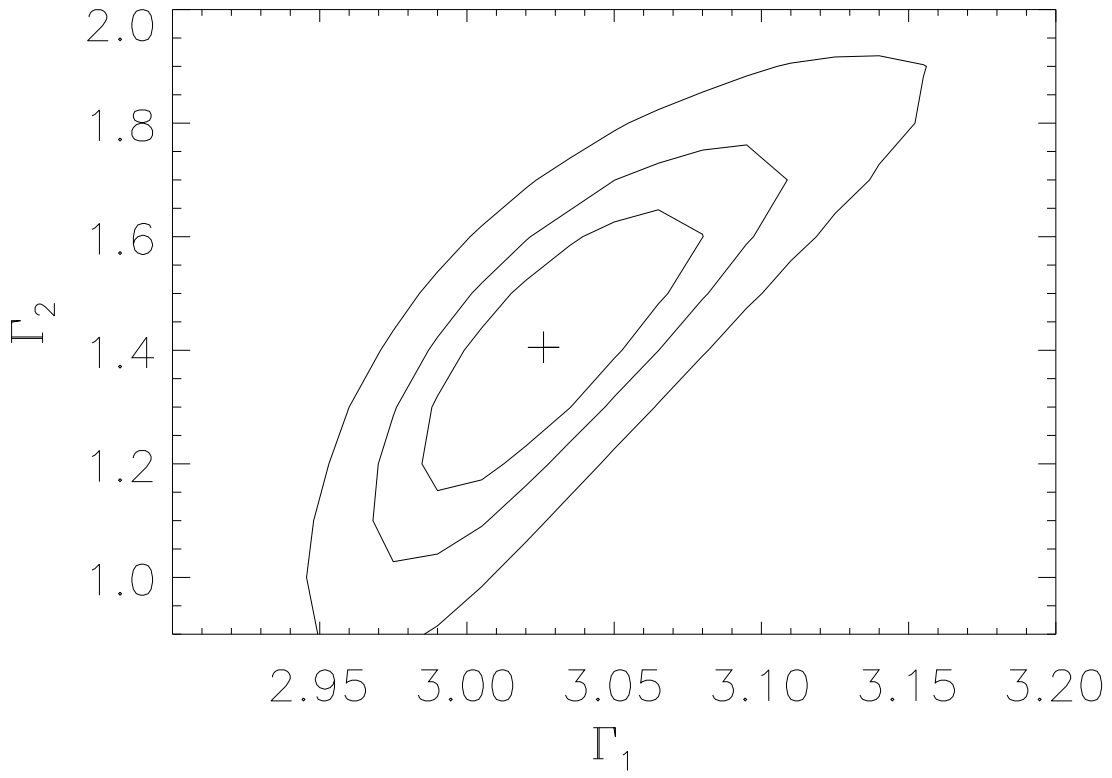

Fig. 4.— The confidence region for the two spectral slopes fitted to the LETGS and MECS data. The contours give 1σ, 90% confidence, and 99% confidence for the two parameters jointly.

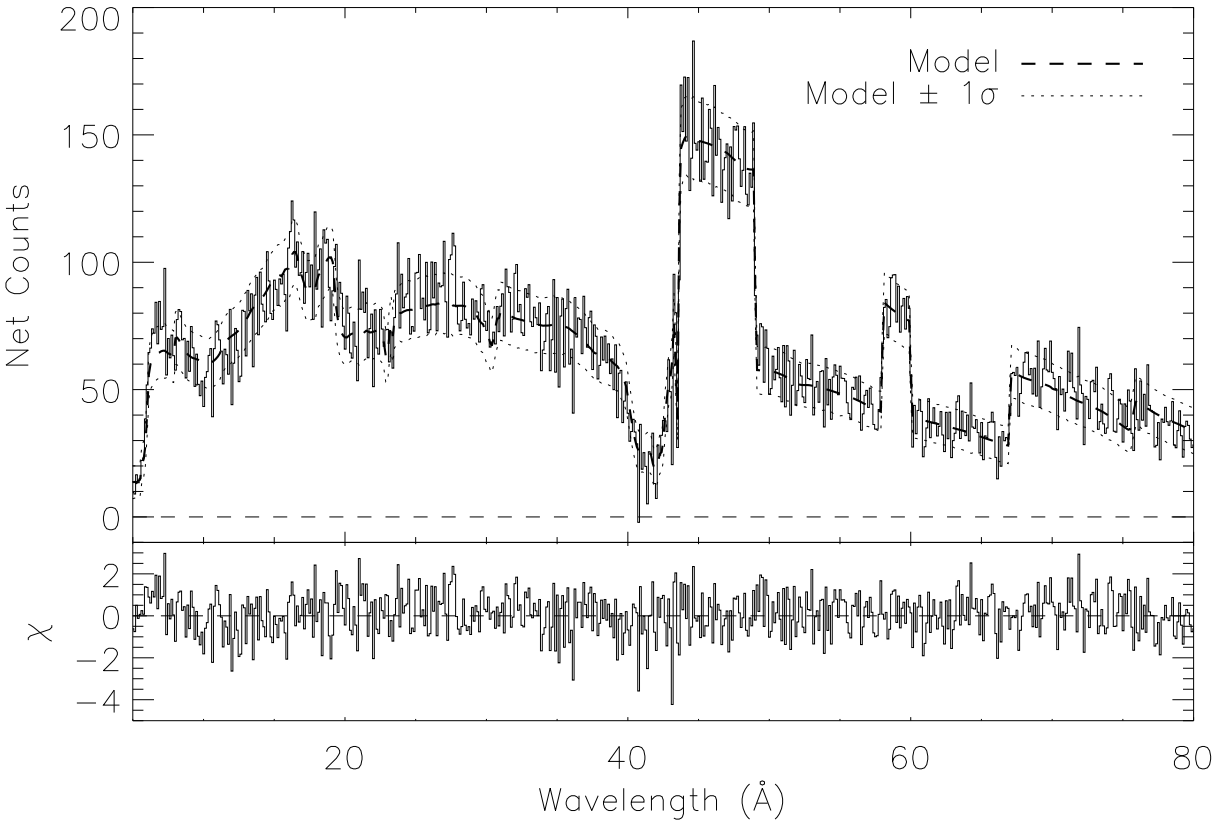

Fig. 5.— *Top:* The count spectrum of Mrk 478 obtained with the LETGS. *Bottom:* Residuals from the best fit power law model. A binning of 0.125Å was used to obtain sufficient signal per bin to search for narrow features. *Heavy dashed line:* expected count spectrum from a steep power law fitted to the data shown in figure 2. *Light dotted lines:* $\pm$ 1 σ uncertainties about the model. The residuals are generally consistent with statistical fluctuations about the model. The sharp edges in the model near 50 and 60Å are due to detector gaps. The only feature with sufficient significance ($> 4\sigma$) is a result of poor modelling of the instrumental C-K edge near 43.2 Å.

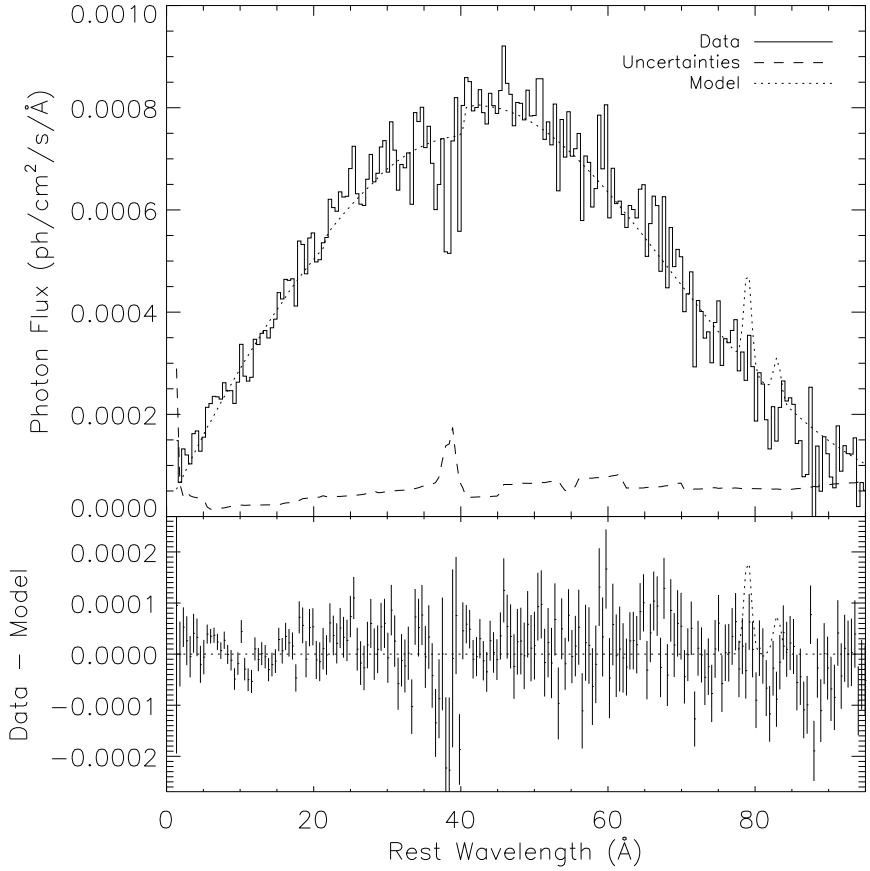

Fig. 6.— The first order spectrum of Mrk 478 binned at 0.5Å (top panel) and the residuals from the best fit power law model (bottom panel), excluding the lines. The contributions from orders 2-5 have been subtracted using the power law spectral model and the efficiencies derived from the calibration observation of PKS 2155-304. Residuals near the C K edge in first order result from systematic errors in the effective area calibration. No broad lines are detected. By way of illustration, the lines claimed by Hwang and Bowyer (1997) on the basis of EUVE data are included in the model in the top panel (but not used to calculate the residuals in the bottom panel). It is also clear that the 75-100 Å continuum is not dominated by emission lines, contrary to the claim of Hwang and Bowyer (1997).

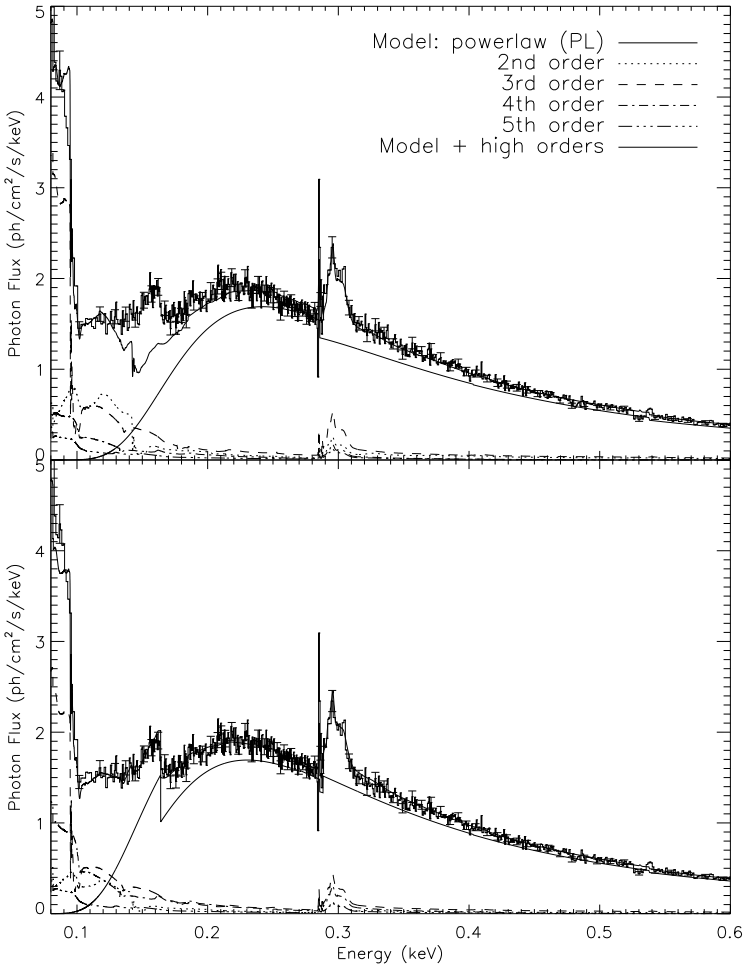

Fig. 7.— The LETGS spectrum of PKS 2155-304 taken from observation 331, used to assess the LETGS calibration at low energies. The bin sizes have been varied to provide a signal/noise ratio of 20 in each bin. *Top panel:* Spectrum computed using eq. A2 and the LETGS calibration files as referenced in the appendix. High orders are computed using the fitted model and eq. A4. Several problems are very clear: 1) a continuum mismatch across the C-K edge (0.285 keV), 2) a jump at 0.162 keV, 3) the 2nd order C-K edge is too large, and 4) the 3rd order C-K edge is slightly too large. *Bottom panel:* The spectrum was computed the same way but adjustments to the high orders have been included as described in the appendix. Two features have been modelled as model edges – at 0.285 and 0.162 keV – and then applied to the first order effective area. The result is a very good fit to the overall spectrum from 0.08 to 0.6 keV.

Table 1. Spectral Fit Parameters

Data Set	N_H (10^{19} cm^{-2})	K_1 (ph cm^{-2} s^{-1})	Γ_1	K_2 (ph cm^{-2} s^{-1})	Γ_2	χ^2(dof)
LETGS and MECS	9.8±0.3	3.32±0.22 $\times 10^{-3}$	3.03±0.04	0.28±0.24 $\times 10^{-3}$	1.4±0.2	216(150)
LETGS only	9.1±0.3	3.75±0.07	2.91±0.03	···	···	81.6(52)
MECS only	9.8(f)	2.0±0.2	2.19±0.05	···	···	110.9(98)
LETGS and MECS	2.6±1.4	3.63±0.06	2.79±0.02	···	···	439(152)

Note. — Uncertainties are 90% confidence values for 1 interesting parameter for a model of the form $n_E = e^{-N_H \sigma(E)}[K_1 E^{-\Gamma_1} + K_2 E^{-\Gamma_2}]$, where $\sigma(E)$ is the energy-dependent cross section for interstellar material of cosmic abundances. Only one power law is fitted to the LETGS or MECS data in isolation. An "f" indicates where the N_H was fixed. The number of degrees of freedom in the fit is given in parentheses.